PERGAMON

European Journal of Cancer 38 (2002) 1278–1287

European Journal of Cancer

www.ejconline.com

Therapy of rat tracheal carcinoma IC-12 in SCID mice: vascular targeting with [^{213}Bi]-MAb TES-23

S.J. Kennel[a,*], T. Lankford[a], S. Davern[a], L. Foote[a], K. Taniguchi[b], I. Ohizumi[b], Y. Tsutsumi[c], S. Nakagawa[c], T. Mayumi[c], S. Mirzadeh[a]

[a]*Life Sciences Division, Oak Ridge National Laboratory, Oak Ridge, TN 37831-6101, USA*
[b]*Fuji Gotemba Research Laboratories, Chugai Pharmaceutical Co., Ltd., Shizuoka 412-8513, Japan*
[c]*Department of Biopharmaceutics, School of Pharmaceutical Sciences, Osaka University, Suita, Osaka 565-0871, Japan*

Received 16 October 2001; received in revised form 8 January 2002; accepted 20 February 2002

Abstract

In previous work, we have demonstrated that vascular targeting of [^{213}Bi], an α-emitter, to lung blood vessels could efficiently destroy tumour colonies growing in the lung. In order to expand this approach to treatment of tumours growing in other sites, we employed the monoclonal antibody (MAb) TES-23, which reacts with CD44H, preferentially expressed on new blood vessels in tumours. Biodistribution studies of *N*-succinimidyl [^{125}I] 3-iodobenzoate (SIB)-radiolabelled MAb TES-23 in ICR-severe combined immunodeficient (SCID) mice bearing subcutaneous (s.c.) and intramuscular (i.m.) IC-12 tumours, demonstrated efficient tumour uptake. At 24 h, accumulation in small tumours was 45%ID/g for s.c. tumours, and 58%ID/g for i.m. tumours and in large tumours it was 25%ID/g for s.c. tumours and 17%ID/g for i.m. tumours. Micro-autoradiography data confirmed that radiolabel accumulated in or near tumour blood vessels. Normal tissues had very low levels of radioactivity. Treatment of mice bearing small IC-12 tumours with [^{213}Bi] MAb TES-23 retarded tumour growth relative to animals treated with cold MAb TES-23. Biodistribution and therapy experiments were also performed in BALB/c mice bearing both s.c. and i.m. syngeneic, lung carcinoma (line 498) tumours. [I^{125}] SIB MAb TES-23 accumulated efficiently in both s.c. and i.m. tumours (14%ID/g and 15%ID/g, respectively, at 4 h); however, no therapeutic effect of [^{213}Bi] MAb TES-23 treatment could be demonstrated in this model system. The data demonstrate that the timing of vascularisation of the tumours and the delivery kinetics of MAb relative to the half-life of the therapeutic radionuclide are critical for effective therapy. © 2002 Published by Elsevier Science Ltd.

Keywords: TES-23, [^{213}Bi]; Vascular targeting; Therapy; SCID mice

1. Introduction

Much recent research in cancer therapy has been focused on tumour vasculature [1]. The majority of this work is directed at the inhibition of formation of new tumour blood vessels, usually termed anti-angiogenesis therapy [1–3]. Anti-angiogenesis therapy has shown tremendous promise and the current challenge is to extend remission times to the point that tumour cells die and continuing treatment is not necessary [4].

Vascular targeted radioimmunotherapy (VT-RAIT), has the potential to kill both tumour blood vessels and adjacent tumour cells [5,6]. VT-RAIT also has the advantage of rapid and efficient delivery of radionuclides to the tumour site [6], which is in contrast to the conventional approach of tumour-cell-targeted radioimmunotherapy wherein the accumulation of radioisotope at the tumour site is limited by extravasation of the targeting agent [7]. The use of smaller targeting agents [8–10] and two-step targeting [11–13] are current approaches aimed at solving this problem.

VT-RAIT has been shown to be effective in a model system in which we have targeted radionuclides to lung blood vessels serving lung tumour colonies [14–16]. Alpha emitters are well suited to VT-RAIT due to their high linear energy of transformation (LET) and short half-life. The most effective radioisotope which has been used to date is the alpha emitter, [^{213}Bi] [14]. The short path-length of the alpha particle limits damage to untargeted, adjacent tissue [15,17], but also limits VT-

* Corresponding author. Tel.: +1-865-574-0825; fax: +1-865-576-7651.
E-mail address: kennelsj@ornl.gov (S.J. Kennel).

0959-8049/02/$ - see front matter © 2002 Published by Elsevier Science Ltd.
PII: S0959-8049(02)00078-3

RAIT therapy of small tumours in which cells are within approximately 80–100 μm of the targeted blood vessel [6]. Although the lung model system has been useful to demonstrate the principle of VT-RAIT, this approach does not address the issue of VT-RAIT for tumours growing at different sites in the body. Targeting agents selective for tumour vasculature must be found in order for VT-RAIT to be effective for solid tumours and their metastases. A number of these agents have been identified which have some promise for selective targeting [18–22]. The monoclonal antibody (MAb) TES-23 [23–26] has the most desirable homing properties. A rat tracheal carcinoma, IC-12, has been studied in our lab as a model tumour that induces the synthesis of new blood vessels when transplanted into severe combined immunodeficient (SCID) mice. It produces large amounts of the angiogenic factor, fibroblast growth factor-β (data not shown). Vessels invading the tumour are produced when the tumour is implanted at different anatomical sites; however, it is not known if antigenic expression varies in vessels induced at different sites. The new blood vessels are present in the tumour as soon as 4–5 days after tumour cell injections, thus providing a good model system for therapeutic targeting to the tumour vasculature.

2. Materials and methods

2.1. MAb radiolabelling and documentation

MAb TES-23 was isolated from hybridomas formed with spleen cells from BALB/c mice immunised with tumour endothelial cells isolated from KMT-17 fibrosarcomas grown in WKAH rats (23). Control MAb 20a is a BALB/c IgG MAb that reacts with a mycoplasma protein, but does not react with any normal mouse or rat protein.

Two methods of radioiodination were used. For western blot detection, MAb TES-23 was radioiodinated with carrier free [^{125}I] (Amersham Pharmacia Biotech) using the Chloramine T method and purified by gel filtration [27]. This method is useful for labelling to high specific activities. In order to minimise dehalogenation, radioiodination for cell binding and biodistribution studies was done with the succinimidyl iodobenzoate (SIB) method [28]. *N*-succinimidyl 3-(trimethylstannyl)-benzoic acid MeATE, was synthesised and purified by the method of Koziorowski and colleagues [29] and was dissolved in methanol containing 5% glacial acetic acid. MeATE (0.2–1.0 μg in 2 μl) was added to carrier free [^{125}I] (1–20 μl in dilute NaOH) and 5 μg of Chloramine T was added in 5 μl of water. The reaction was stopped after 5 min at 40 °C by addition of 1 ml of 1 mg/ml sodium metabisulphite and the mixture was transferred to a syringe barrel attached to a Sep-Pak C18 cartridge (Waters). Two ml of water was added and the solution was pushed through the cartridge. The resin was washed with 5 ml of water and the [^{125}I]-succinimidyl iodobenzoate ([^{125}I] SIB) was eluted with pure methanol. The methanol solution was evaporated to dryness under a stream of air and the residue was dissolved in 200 μl acetonitrile. The solvent was evaporated again and the [^{125}I] SIB, judged to be $>75\%$ pure by thin layer chromatography (TLC), was dissolved in 5 μl of 0.5 M sodium borate buffer (pH = 8.6) and added directly to purified, concentrated antibody in 0.01 M Na phosphate buffer (pH 7.6) in 0.15 M NaCl (0.01 M sodium PO_4, pH 7.6 with 0.15 M NaCl (PBS)). The reaction was quenched after 10 min at 37 °C by the addition of 0.1 M glycine. IgGs radioiodinated with SIB were purified by gel filtration on Utragel AcA 34 resin in PBS containing 0.1% gelatin [30]. All radioiodinated antibodies were analysed on sodium dodecyl sulphate-polyacrylamide gel electrophoresis (SDS-PAGE) followed by autoradiography to confirm the incorporation of [^{125}I] and the purity of the product (data not shown).

MAb TES-23 and control MAb 20a were radiolabelled with [^{213}Bi] as previously described in Ref. [14]. Briefly, the antibodies were reacted with bifunctionalised cyclohexyl diethylenetriamine pentaacetic acid CHX-A″ DTPA [31,32] and freed of excess reagent and metals by dialysis. The products were found to have 0.7–1.0 active chelate sites per antibody molecule [33]. Bi-213 was eluted from a [^{225}Ac] resin bound generator with 0.15 M HI and the neutralised [^{213}Bi] coupled to CHX-A″ DTPA MAb for 6 min at room temperature. Incorporation of [^{213}Bi] was greater than 90% in all cases as judged by retention in Microcon 30 filter units (Millipore Corp., Bedford, MA, USA). The [^{213}Bi] conjugated antibodies were used without further purification. All radioconjugates were found to contain $<0.001\%$ residual [^{225}Ac]. In some experiments, [^{213}Bi] MAbs were analysed on SDS-PAGE. [^{213}Bi] was incorporated into the heavy and light chains of the antibodies in approximately equal amounts (data not shown).

2.2. Cell binding and western blots

IC-12 [34], 498 [35], LEII [36], or MLEC [37] cells were grown to confluence in flat-bottom, 96-well snap-apart plates. The cells were fixed with 0.5% gluteraldehyde in PBS and unreacted sites were saturated with 5 mg/ml bovine serum albumin (BSA) in PBS. Radiolabelled antibodies were added in 50 μl of the same solution and incubated with rotation for 3 h at room temperature. Wells were washed free of unbound radioisotope and analyzed for radioactivity in a Cobra Quantum gamma spectrometer (Packard). Data were analysed as previously described in Ref. [38].

For western blot, cell membrane lysates were prepared as previously described in Ref. [27]. Briefly, cells

or tissues were homogenised in PBS containing protease inhibitors and the crude membrane fraction collected by centrifugation for 10 min at 10 000*g*. The pellet was suspended and homogenised in the PBS-protease inhibitor solution, but containing 0.5% Nonidet (N)P40. The solutions were centrifuged as before and the soluble fraction was used for western blotting [27]. Polyacrylamide gels (8%) were used to separate proteins loaded in 1% SDS, 8 M urea without reducing agent added. Addition of a reducing agent was found to destroy reactivity with MAb TES-23. Separated proteins were transferred to Immobilon P membranes and probed with 100 ng/ml [^{125}I] MAb TES-23 (10 μCi/μg) for 2 h at room temperature. Washed blots were subjected to phosphorimager analysis on a Cyclone instrument (Packard Instrument Company).

2.3. Biodistribution, micro-autoradiography and therapy

All animal experiments were performed according to protocols approved by the ORNL animal care and use committee (protocol #0256). ICR-SCID female mice were obtained from Taconic Farms at 4 weeks of age and used before they were 12 weeks old. The mice were injected subcutaneously (s.c.) and intramuscularly (i.m.) with 10^6 IC-12 cells in 50 or 100 μl PBS [14]. Similarly, BALB/c mice were injected with 10^5 498 cells. At appropriate times, animals were used for biodistribution studies or therapy.

All biodistribution experiments were done with [^{125}I] SIB-labelled MAb to minimise the loss of [^{125}I] from the antibodies due to dehalogenation. Animals bearing small (8 days of growth) or large (12 days of growth) IC-12 tumours were injected intravenously (i.v.) with 0.5 μg MAb TES-23 containing 2.5 μCi of [^{125}I] in 200 μl of PBS with gelatin carrier protein. Two animals each were sacrificed after 1, 4 or 24 h, and 15 organs as well as tumours growing s.c. or i.m. were removed, weighed and analysed for radioactivity. A similar experiment was performed with 2.0 μg of [^{125}I] SIB MAb TES-23 (1.4 μCi) injected into BALB/c mice bearing 498 lung carcinomas in s.c. and i.m. sites. Data were corrected for counter background and the values for %ID/g±standard error were calculated for each tissue.

At 24 h postinjection, animals were sacrificed for microdistribution studies. Several tissues and both tumours were removed and fixed in 10% buffered formalin for 24 h. The fixed tissue was washed in PBS and processed for paraffin sectioning at 6 μm per section. In the IC-12 experiment, frozen sections were prepared from one animal as well. The slides containing the tissue sections were dipped in NTB emulsion (Kodak) and stored in the dark for 3–6 weeks. The emulsion was developed and the tissue was stained with haematoxylin and eosin before mounting in Permount. Images were captured from a Nikon microscope with a Sony CCD camera using Photoshop software on a Power Macintosh computer.

In therapy experiments, animals were treated i.v. with 200 μl [^{213}Bi] CHX A″-DTPA TES-23 (10–20 μg per injection) with 166–240 μCi [^{213}Bi]. Controls consisted of [^{213}Bi] MAb 20a or of [^{213}Bi] complexed with DTPA and mixed with the non-chelate form of MAb TES-23. Animals were observed daily and tumours were graded for size by three investigators. Due to the irregular shape of the multilobed tumours, tumour burden was estimated by a grading system. The approximate tumour sizes were: grade 1: 0.1 g; grade 2: 0.2–0.3 g; grade 3: 0.4–0.6 g; and grade 4: 0.7–1.0 g. According to our animal care protocol, animals were sacrificed when tumours approached 1.0 g in size or when ulcerated skin was apparent.

3. Results

3.1. MAb TES-23 radiolabelling and characterisation

The source [23,24], purification [24] and target antigen, CD44H, [25,26] for MAb TES-23 have been described previously. For all biodistribution studies described herein, we conducted radioiodination of the antibody using the [^{125}I] SIB reagent [28]. This method attaches a para iodo-benzoyl group through an amide linkage to free amino groups of the antibody [29]. Radioiodination was performed in this way to produce labeled MAb with higher resistance to dehalogenation *in vivo* [28,30]. Analysis on PAGE indicated that >95% of the [^{125}I] SIB was attached to either the heavy or light chains of the antibody (data not shown). Direct binding of the [^{125}I] MAb TES-23 to cultured cells fixed in 96-well plates was evaluated. The antibody bound to rat tracheal carcinoma cells, IC-12, with a $Ka = 1.1 \times 10^9$ M^{-1}. A maximum of 60% of the radiolabel was bound to the cells and saturation binding indicated that each cell had approximately 380 000 binding sites (data not shown). No significant binding could be detected with any mouse cell lines including carcinomas cells 498 and EMT-6 or endothelial cell lines LEII or MLEC. Western blot analysis to identify the target antigen in membrane proteins of cells and tissue was done with [^{125}I] MAb TES-23 radioiodinated using the Chloramine T method. Autoradiograms shown in Fig. 1 demonstrate bands at approximately 95 kDa, corresponding to the size of CD44H, for lanes containing proteins from IC-12 cells and also from IC-12 tumour after growth in SCID mice. No bands were detected in western blots of proteins from membranes of cells from four other cell lines or from 19 normal murine tissues. Although MAb TES-23 accumulated in murine 498 carcinoma tumours (see below), no bands could be detected in western blots

of proteins from this cell line or from 498 tumours grown in BALB/c mice.

MAb TES-23 was reacted with bi-functional CHX-A″-DTPA at a molar ratio of 17:1. This reagent reacts with antibody at free amino groups in a fashion similar to the reaction used for radioiodination with [^{125}I]-SIB. Quantitation of metal binding in a standardised assay [33] indicated that an average of 0.7 active chelator groups were attached per antibody molecule. The preparation was tested for incorporation of [^{213}Bi] via the standard reaction conditions. Up to 90% of the added [^{213}Bi] could be complexed to antibody, yielding specific activities greater than 10 μCi/μg protein. Polyacrylamide gel analysis showed that freshly prepared [^{213}Bi] MAbs had radiolabel associated with both heavy and light chains, but that when gel separation was delayed by several hours, radiolabel was observed at the gel front, indicating dissociation from MAb. The dissociated radioactivity was ascribed to [^{209}Pb], a β-particle emitter, which is a decay daughter of [^{213}Bi] and is known to be released from the chelator (data not shown).

3.2. Biodistribution and microdistribution of [^{125}I] SIB MAb TES-23

The biodistribution of radioiodinated MAb TES-23 was evaluated in mice bearing IC-12 tumours. Data were collected for small (day 8 after cell injection) and large (day 12 after cell injection) IC-12 tumours growing both s.c. and i.m. in ICR-SCID mice. Several points should be noted from the data (Fig. 2a and b). MAb TES-23 accumulated to relatively high concentrations in both s.c. and i.m. IC-12 tumours indicating that antigen expression and availability were similar at both sites. The specific MAb concentration was higher in the smaller tumours than in the larger ones (compare Fig. 2a and b). Accumulation increased over time from 1 to 24 h for tumours in all data sets. The blood contained high levels of radioiodinated antibody at 1 and 4 h postinjection, but the levels diminished by 24 h. Finally, radioactivity detected in the thyroid was low, indicating that little dehalogenation of [^{125}I] SIB MAb TES23 had occurred during the time course of the experiment.

At 24-h postinjection of [^{125}I] MAb TES-23, tumour and normal tissues were collected and samples fixed and embedded in paraffin. Six-μm sections were cut in preparation for autoradiography. Autoradiograms of these sections are shown in Figs. 3 and 4. Small IC-12 tumours growing s.c. (Figs. 3a) or i.m. (Fig. 3b) both showed relatively high, but uneven distribution of [^{125}I] (black silver grains), whereas normal tissue including liver (Fig. 3c), lung (Fig. 3d), spleen (Fig. 3e) and kidney (Fig. 3f) had little detectable [^{125}I]. Higher magnification of the tumour section autoradiograms (Fig. 4a and b) showed that the [^{125}I] had a perivascular microdistribution. In Fig. 4b, some muscle cells can be seen as the tumour invades this tissue. Little [^{125}I] was seen in the muscle; however, the radioisotope was found in the extracellular space between the tumour and muscle cells.

A similar set of experiments was performed for the biodistribution and microdistribution of the radioiodinated antibody in BALB/c mice bearing s.c. and i.m. tumours derived from the syngeneic adenocarcinoma line 498 cells. Data in Fig. 5 show that accumulation of [^{125}I] in 498 tumours was about 3-fold lower than for accumulation in IC-12 tumours. In addition, the accumulation did not increase from 1 to 24 or even 72 h postinjection as had been observed for the IC-12 tumours (Fig. 2a and b). Concentrations in normal BALB/c organs were similar to those seen in the ICR-SCID mice bearing IC-12 tumours. Autoradiography of tissue sections showed a slightly higher grain density in tumour tissue than in normal tissue in these animals, but the microdistribution could not unambiguously be assigned to the blood vessel sites (data not shown).

3.3. Radioimmunotherapy

ICR-SCID mice bearing both s.c. and i.m. tumours were treated with 160–170 μCi [^{213}Bi] MAb TES-23, [^{213}Bi] control MAb 20a, or MAb TES-23 without [^{213}Bi]. Tumour size was graded daily without knowledge of the treatment groups. Data in Fig. 6 show that tumours in animals treated with the specific [^{213}Bi]-labelled MAb TES-23 grew more slowly than those in animals treated with cold MAb TES-23. Growth in animals treated with [^{213}Bi] control MAb 20a was

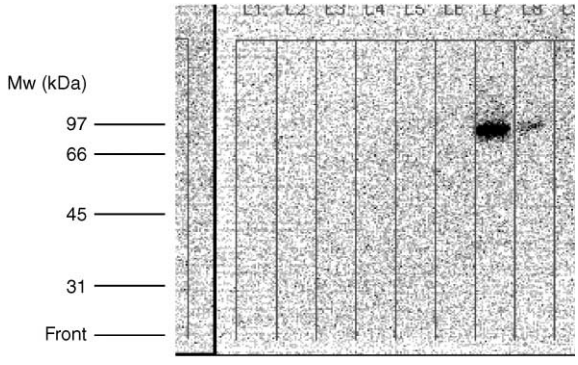

Fig. 1. Autoradiograms of western blots developed with [^{125}I] MAb TES-23. Detergent solubilised proteins (10 μg/lane) from membrane preparations of cells and tissues were separated on 8% acrylamide SDS-PAGE and transferred to Immobilon membranes. Blots were probed with 100 ng/ml of [^{125}I] MAb TES-23 at 1 μCi/μg. Probed membranes were washed and exposed to a Phosphor Imager screen for 20 min. Lanes 1–9 contain proteins from: heart, lungs, uterus and ovaries, thymus, adrenal, LEII cells, IC-12 cells, IC-12 tumour, and EMT-6 cells, respectively. Specific labelling was detected in lanes 7 and 8 only.

intermediate between the other two groups. Tumour growth progressed in all animals until they had to be sacrificed according to the procedures dictated by our approved animal care protocol.

BALB/c mice bearing either i.m. or s.c. tumours from the rapidly growing, syngeneic lung adenocarcinoma 498 cells were treated with 240 μCi of either [^{213}Bi] MAb TES-23, [^{213}Bi] control MAb 20a or [^{213}Bi] mixed with, but not coupled to, MAb TES-23. No difference in tumour growth among the animals with i.m. tumours was noted (data not shown). Two of five animals in the group with s.c. tumours treated with [^{213}Bi] MAb TES-23 had slightly slower tumour growth. In an attempt to verify this apparent therapeutic effect, the experiment was repeated with 10 animals per group. No difference in the tumour growth patterns among the treatment groups was noted and all animals had progressing tumours at the time of sacrifice.

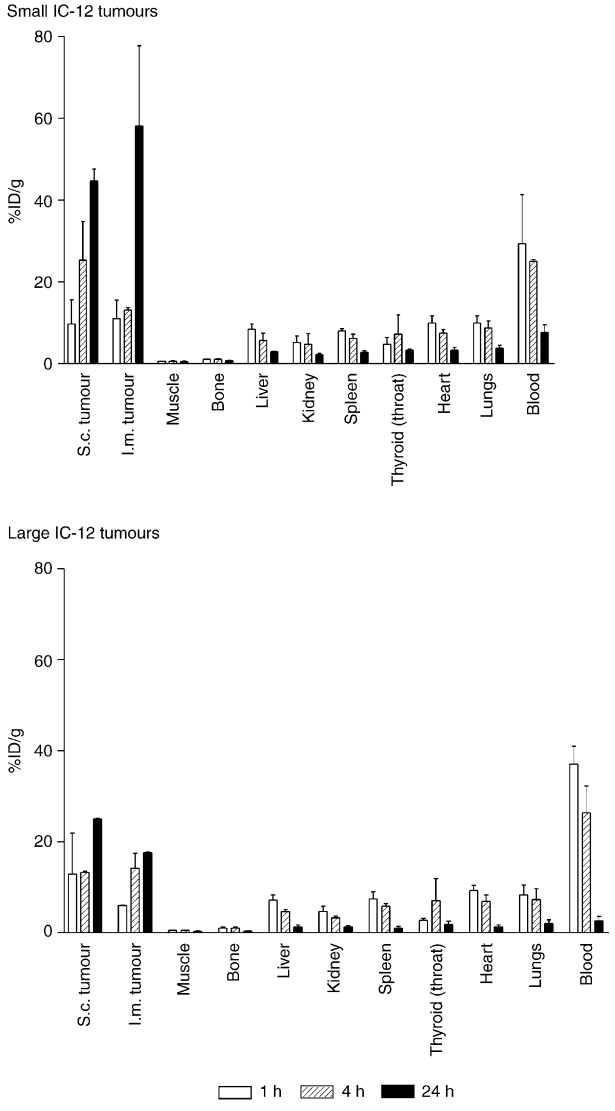

Fig. 2. Distribution of [^{125}I] SIB MAb TES-23 in ICR-SCID mice bearing s.c. and i.m. tumours. Small tumours (panel a) at day 8 post-injection were 0.06±0.04 g for s.c. tumours and 0.22±0.07 g for i.m. tumours. The larger tumours (panel b) were grown for 12 days and were 0.27±0.15 g for s.c. and 0.90±0.43 g for i.m. tumours, respectively. All animals were injected with 200 μl containing 12 μg of radiolabelled antibody (1.0 μCi/μg). Values are expressed as %ID/g±S.E. for two mice per data point. h, hour.

4. Discussion

Radioimmunotherapy trials of solid tumours which utilise MAb targeted to antigens on the tumour cell surface have not proven successful in many cases due to the low fraction of the injected dose of radioisotope that accumulates at the tumour site [7]. This is due, in part, to the relatively poor ability of antibody carriers to penetrate the blood vessel walls. In addition to the amount of the injected dose that accumulates at the tumour site, the kinetics of accumulation must be coordinated with the half-life of the radioisotope. Certainly, penetration of the vessel walls and tumour in a short time-frame is an issue, with short-lived radioisotopes such as [^{213}Bi] ($t_{1/2}$ = 46 min). Even with this constraint, the properties of high LET and short path-length of the alpha particle make [^{213}Bi] an attractive radioisotope for small tumour therapy. Two therapy studies have been reported with [^{213}Bi] coupled to antibody fragments targeted to antigens expressed on the surface of solid tumours [9,17]. In one of these studies, some therapeutic effect was noted, but it was concluded that the accumulation needed to be faster to take full effect of the decay of [^{213}Bi]. In addition, another group reported a significant increase in survival time using [^{213}Bi] complexed with an IgG MAb to treat animals bearing prostate cancer xenografts i.m. [39].

We have been exploring VT-RAIT as an alternative to the classical radioimmunotherapy. In VT-RAIT, the tumour vessel is the target for radiolabelled antibody. Since the binding site for the antibody is in the lumen of the blood vessel, accumulation of the injected dose is relatively efficient [6,14,24]. We have demonstrated this efficient targeting and the therapeutic effect of [^{213}Bi] and other radioisotopes targeted to lung blood vessels serving lung tumour colonies [6,14,15,30,40]. Although work in our lung model system represents the first step in demonstrating the usefulness of VT-RAIT, more realistic models must be developed.

VT-RAIT will be effective for the treatment of micrometastasis only if tumour vessels in different anatomical sites can be recognised by a single targeting agent. It is generally thought that tumour vascularisation occurs as a result of the induction of new vessels growth as an extension or recruitment of vessels from the adjacent normal tissue. If this is the case, it is possible that the new vessels would have characteristics unique to the host normal tissue. Expression of any

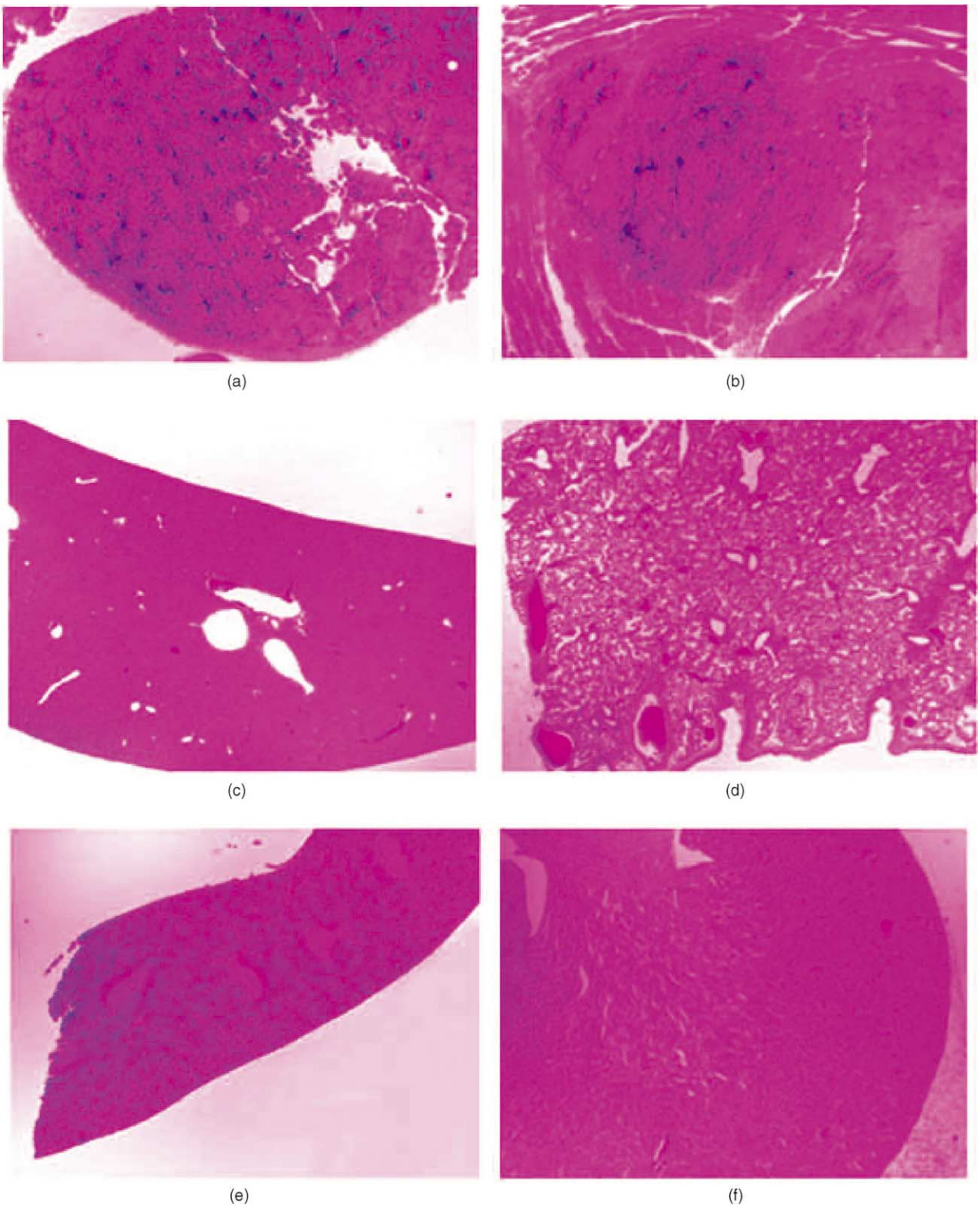

Fig. 3. Autoradiography of tissue sections harvested from ICR-SCID mice with small IC-12 tumours as described for Fig. 2. Slides were exposed to emulsion for 3 weeks before developing. Images were captured with a 2× objective using a Sony video camera. Black grains represent localisation of ^{125}I. Panels: (a) s.c. tumour; (b) i.m. tumour; (c) liver; (d) lung; (e) spleen; (f) kidney.

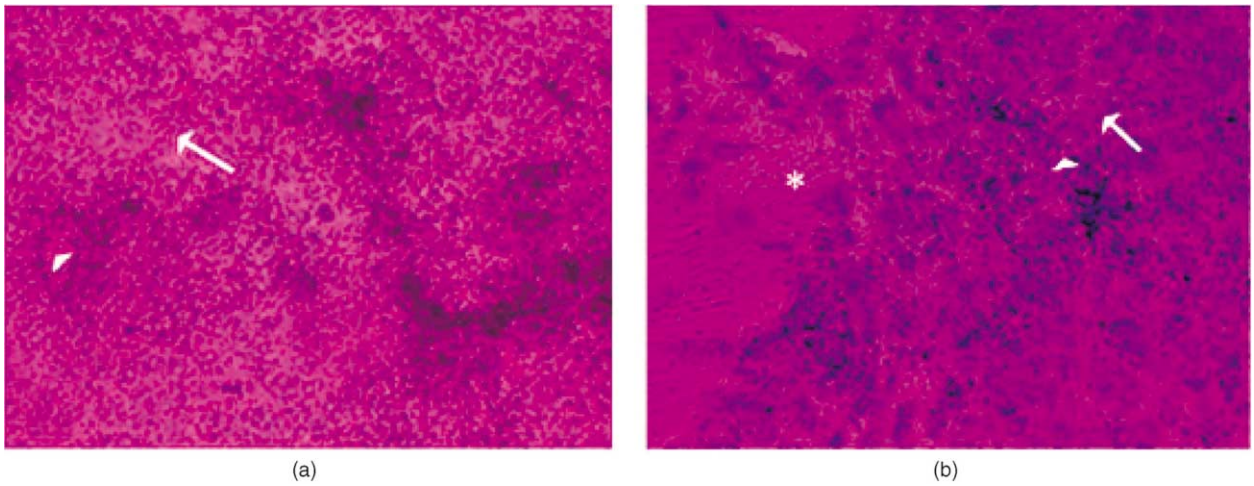

Fig. 4. Autoradiography for samples described in Fig. 3. Lens objective was 40×. Panel (a), s.c. tumour and panel (b) i.m. tumour. The arrowheads designate red cells in blood vessels, the arrows point to tumour cells and the star is on a muscle cell.

target antigen in the tumour blood vessel thus may vary depending on the site at which the tumour is growing. For this reason, our test system included IC-12 tumours growing at different sites.

We have tested several antibodies and peptides for their homing properties to tumour vessels in a mouse model of s.c. and i.m. tracheal carcinoma tumours (IC-12) growing in SCID mice. The hypothesis is that an antibody that can recognise tumour endothelium at different sites (vascular beds) in the animal might be capable of treating micrometastases of the tumour no matter what organ site in which they may be growing. To date, MAb TES-23 which reacts with rat CD44H [25,26] demonstrated the best homing properties among the reagents tested. Recent reports indicate that this antibody may recognise two antigens [26].

In our system, western blot analyses indicate that CD44 is the major antigen recognised (see Fig. 1). CD44 was detected in IC-12 cells grown in tissue culture, as well as in the IC-12 tumours grown in mice. Western blot data could not distinguish if the CD44 recognised was from the tumour cells or the blood vessels in the tumour. Our model system uses a rat tumour cell line, IC-12, which grows in immuno-compromised SCID mice, inducing the adjacent mouse tissue to produce new blood vessels. It should be noted that MAb TES-23 was developed by immunisation of a mouse with rat endothelial cells. In our experience [6,38], mouse MAb prepared in this way rarely reacts with murine antigens due to self-tolerance. Consistent with this hypothesis, we were not able to detect reaction in western blot analysis with proteins from any mouse tissues or from mouse tumours growing in syngeneic animals (498 tumours in BALB/c mice).

Two therapy studies have been published which utilised [^{213}Bi] targeted directly to tumour cells with antibody fragments [9,17]. The study with diabodies targeted to SK-OV-3 carcinoma reported little therapeutic effect [9]. In contrast, treatment of human colon tumour xenografts with [^{213}Bi] CO17-1A Fab′ demonstrated very good therapy, including cures of liver metastases of GW39 tumours [17]. Another study showed retardation of growth of prostate cancer xenografts when treated with a [^{213}Bi] MAb to the tumour cells [39]. The differences among these results may be the kinetics of accumulation and penetration at the tumour site. [^{213}Bi] CO17-1A Fab′ was shown to localise (~5%ID/g) to the tumour within 10 min–1 h post-injection, which should allow for an efficient transfer of

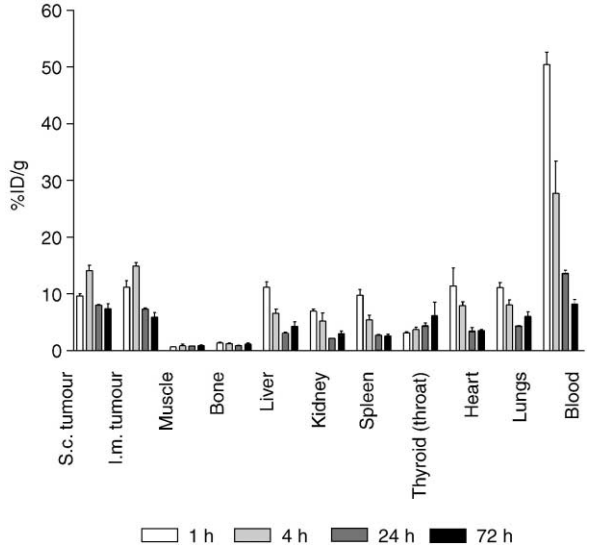

Fig. 5. Distribution of [^{125}I] SIB MAb TES-23 in BALB/c mice bearing either s.c. or i.m. line 498 tumours. For tumours harvested at 1–24 h, both the s.c. and i.m. tumours were approximately 0.2 g each, but by 72 h, the tumours had grown to about 0.6 g/mouse. [^{125}I] SIB MAb TES-23 (1.6 μCi, 2 μg) injected in 0.2 ml of PBS with 0.1% gelatin as carrier protein. Data for two animals per point expressed as %ID/g±S.E. h, hour.

[^{213}Bi] decay energy [17]. The data presented in this work indicate that [^{125}I] MAb TES-23 accumulated very rapidly (~10%ID/g at 1 h) at the site of IC-12 tumour growth, whether the site was s.c. or i.m. (see Fig. 2a and b). This accumulation pattern and the microdistribution data (Figs. 3 and 4) are consistent with TES-23 binding at the tumour blood vessel; however, this point can not be proven at the level of resolution of light microscopy. It is possible that the antibody is binding to tumour cells which are adjacent to the blood vessels. In fact, cell-binding data show that MAb TES-23 does bind very well to IC-12 cells. The data show that the antibody did not bind to murine endothelial cell lines in culture. The absence of binding of endothelial cells in culture does not necessarily indicate that MAb TES-23 does not bind to blood vessels *in vivo*. Endothelial cells in animals have very specialised cell surface compositions which are generally not reflected in similar cell types grown in cell culture [36,37]. This would be expected particularly for a protein preferentially expressed on tumour endothelium.

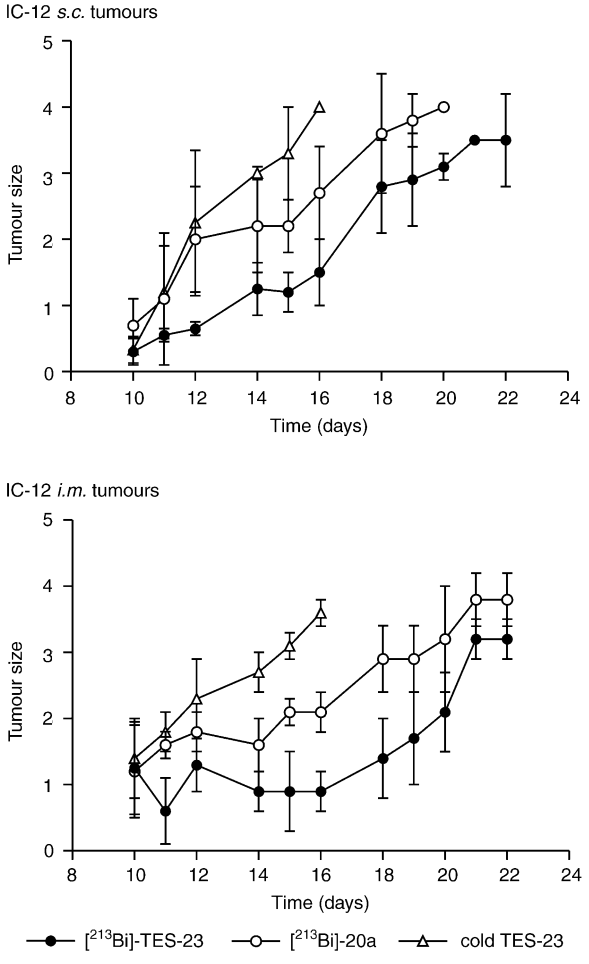

Fig. 6. Therapy of IC-12 tumours growing in ICR-SCID mice. Animals (five per group) bearing tumours of approximately 0.1 g each s.c. and i.m. were injected with 12 μg of MAbs TES-23 or 20a. One group received 166 μCi of [^{213}Bi] MAb TES-23, a second group received 166 μCi of MAb 20a and the third group received cold MAb TES-23 only. Tumours were graded on a scale of 1–4 due to the irregular shape and multiple lobules. Tumour volumes relative to the grading system were: grade 1: 0.1 g; grade 2: 0.3 g; grade 3: 0.6 g; and grade 4: 1 g. Animal protocol #0256 requires that all animals bearing necrotic tumours or those with tumours greater than 1 g should be sacrificed.

No matter what the target antigen may be, MAb TES-23 has the target binding specificity necessary for efficient delivery of a therapeutic radionuclide. The short half-life alpha particle emitter, [^{213}Bi], requires that target binding be very rapid. MAb TES-23 homes to the tumour site more rapidly (10% ID/g at 1 h and 25% ID/g at 4 h) than most antitumour IgGs, presumably due to the fact that it is binding to blood vessels. The accumulation is not as rapid as that observed in the lung blood vessel targeting model where antibody accumulates to maximum values within minutes after injection [14]. The kinetics of antibody accumulation at the site of IC-12 tumours are not rapid enough to deliver the majority of the dose of [^{213}Bi] to the tumour. Nevertheless, targeting of [^{213}Bi] with MAb TES-23 to IC-12 tumours produces a measurable therapeutic effect (Fig. 6). At the time of treatment (7 days posttumour implant), the tumour sizes are at least 2 mm. This may have been too large for curative therapy with the short path-length alpha emitter. Extensive knowledge about the tumour/vessel structure and exact position of the radioisotope relative to the tumour cells is necessary to determine if all cells in the tumour would receive a lethal dose of alpha particles. Computer image capture of cell and radioisotope positions coupled with Monte Carlo calculations of alpha particle track trajectories can be used to estimate the fraction of cells that remain 'unhit' [41]. This microdosimetry approach will be necessary to evaluate any alpha particle-mediated therapy. It is interesting that in these studies, as with others involving both α- [9,14,17,30,40] and β-emitting [15,17,42] radioisotopes, some therapeutic effect is noted with radioisotopes complexed with control targeting agents. This effect seems to be more pronounced with α-emitters, especially those which remain in the circulation for longer times, than with other control treatments [14,30,40]. The effect may be due to oxidative intermediates [43] generated in the circulation, which may be preferentially taken up by or toxic to tumour tissue.

Biodistribution and therapy experiments were also performed with another tumour, 498 lung carcinoma, growing in BALB/c mice. Since 498 cells do not bind MAb TES-23 directly, any specific accumulation of antibody at the tumour site should represent vascular targeting. Biodistribution data show that [^{125}I] MAb TES-23 accumulates at the tumour sites-both s.c. and i.m., (10%ID/g) within 1 h of injection. Furthermore, the amount bound at the tumour site stays relatively constant over a 3-day period. This indicates that initial binding is rapid and saturating as would be expected for vascular targeting. Furthermore, this rapid targeting is

consistent with delivery of the maximum dose possible of the short-half-lived [^{213}Bi]. In spite of these considerations, therapy of 498 tumours with [^{213}Bi] MAb TES-23 was not successful, even though the absorbed dose from [^{213}Bi] should have been similar to that delivered to the IC-12 tumours. It is possible that the extremely rapid growth of the 498 tumour overwhelmed any minor therapeutic effect. As with the IC-12 therapy experiment, tumours were approximately 1–2 mm in size at the start of therapy. Since the position of the tumour blood vessels relative to tumour cells is critical for VT-RAIT utilising the short path-length alpha particle emitters, it is possible that 498 tumour vasculature does not develop as uniformly throughout the tumour as does the IC-12 vasculature (see Fig. 3). In fact, 498 tumours grow so fast that tumour cell-induced angiogenesis may be inconsequential to tumour progression in this model, particularly at early times after implantation.

In summary, it has been shown that MAb TES-23 homes very efficiently to IC-12 tumours growing in SCID mice and that [^{213}Bi] conjugates of the antibody can retard tumour growth significantly. Although tumour targeting of MAb TES-23 to 498 tumours in BALB/c mice was successful, therapy with the [^{213}Bi] conjugate could not be demonstrated. Experiments in both models designed to monitor CD44 H expression locally and high resolution determination of the actual cellular target for MAb TES-23 will be necessary to prove that therapy is mediated by delivery of the radioisotope to blood vessels.

Acknowledgements

The authors thank Arnold Beets for technical assistance. Jim Wesley of Ridge Microtome prepared the sections and performed the autoradiography. Drs Russ Knapp and Brynn Jones were helpful in review of the manuscript. This work was supported by the Department of Energy, Medical Sciences Division, through funding designation ERKP 038. The Oak Ridge National Laboratory is managed by UT-Battelle, LLC, for the US Department of Energy under contract DE-AC05-00OR22725. The submitted manuscript has been authored by a contractor of the US Government under contract DE-AC005-00OR22725. Accordingly, the US Government retains a non-exclusive, royalty-free licence to publish or reproduce the published form of this contribution, or allow others to do so, for US Government purposes.

References

1. Beecken WD, Fernandez A, Joussen AM, *et al*. Effect of anti-angiogenic therapy on slowly growing, poorly vascularized tumors in mice. *J Natl Cancer Inst* 2001, **93**, 382–387.
2. Bergers G, Javaherian K, Lo K-M, Folkman J, Hanahan D. Effects of angiogenesis inhibitors on multistage carcinogenesis in mice. *Science* 1999, **284**, 808–812.
3. Borgstrom P, Hillan KJ, Sriramarao P, Ferrara N. Complete inhibition of angiogenesis and growth of microtumors by anti-vascular endothelial growth factor neutralizing antibody: novel concepts of angiostatic therapy from intravital videomicroscopy. *Cancer Res* 1996, **56**, 4032–4039.
4. Klagsbrun M. Angiogenesis and cancer AACR special conference in cancer research. *Cancer Res* 1999, **59**, 487–490.
5. Denekamp J. Vasculature as a target for tumor therapy. *Prog Appl Microcirc* 1984, **4**, 28–38.
6. Kennel SJ, Mirzadeh S. Vascular targeted radioimmunotherapy with [^{213}Bi]—an alpha particle emitter. *Nucl Med and Biol* 1998, **25**, 241–246.
7. Behr TM, Goldenberg DM, Becker WS. Radioimmunotherapy of solid tumors: a review ''of mice and men''. *Hybridoma* 1997, **16**, 101–107.
8. Yokota T, Milenic DE, Whitlow M, Schlom J. Rapid tumor penetration of a single-chain Fv and comparison with other immunoglobulin forms. *Cancer Res* 1992, **52**, 3402.
9. Adams GP, Shaller CC, Chapell LL, *et al*. Delivery of the alpha-emitting radioisotope bismuth-213 to solid tumors via single-chain Fv and diabody molecules. *Nucl Med Biol* 2000, **27**, 339.
10. Viti F, Tarli L, Giovannoni L, Zardi L, Neri D. Increased binding affinity and valence of recombinant antibody fragments lead to improved targeting of tummoral angiogenesis. *Cancer Res* 1999, **59**, 347–352.
11. Fritzberg AR. Antibody pretargeted radiotherapy: a new approach and a second chance. *J Nucl Med* 1998, **39**, 20N–36N.
12. Axworthy DB, Reno JM, Hylarides MD, *et al*. Cure of human carcinoma xenografts by a single dose of pretargeted yttrium-90 with negligible toxicity. *Proc Natl Acad Sci* 2000, **97**, 1802–1807.
13. Hosono M, Hosonao MN, Kraeber-Bodere F, *et al*. Two-step targeting and dosimetry for small cell lung cancer xenograft with anti-NCAM/antihistamine bispecific antibody and radioiodinated bivalent hapten. *J Nucl Med* 1999, **40**, 1216–1221.
14. Kennel SJ, Boll R, Stabin M, Schuller H, Mirzadeh S. Radioimmunotherapy of micrometastases in lung with vascular targeted ^{213}Bi. *Br J Cancer* 1999, **80**, 175–184.
15. Kennel SJ, Stabin M, Brechbiel M, Mirzadeh S. Treatment of lung tumor colonies with ^{90}Y targeted to blood vessels—comparison with the α-emitter ^{213}Bi. *Nucl Med Biol* 1999, **26**, 149–157.
16. Kennel SJ, Stabin M, Roeske JC, *et al*. Radiotoxicity of Bismuth-213 bound to membranes of monolayer and spheroid cultures of tumor cells. *Rad Res* 1999, **151**, 244–256.
17. Behr TM, Behe M, Stabin MG, *et al*. High-linear energy transfer (LET) alpha versus low-LET beta emitters in radioimmunotherapy of solid tumors: therapeutic efficacy and dose-limiting toxicity of ^{213}Bi- versus ^{90}Y-labeled CO17-1A Fab' fragments in a human colonic cancer model. *Cancer Res* 1999, **59**, 2635–2643.
18. Brooks PC, Montgomery AM, Rosenfeld M, *et al*. Integrin alpha v beta 3 antagonists promote tumor regression by inducing apoptosis of angiogenic blood vessels. *Cell* 1994, **79**, 1157–1164.
19. Demartis S, Tarli L, Borsi L, Zardi L, Neri D. Selective targeting of tumour neovasculature by a radiohalogenated human antibody fragment specific for the ED-B domain of fibronectin. *Eur J Nucl Med* 2001, **28**, 534–539.
20. Epstein AL, Khawli LA, Hornick JL, Taylor CR. Identification of a monoclonal antibody, TV-1, directed against the basement membrane of tumor vessels, and its use to enhance the delivery of macromolecules to tumors after conjugation with interleukin 2. *Cancer Res* 1995, **55**, 2673–2680.
21. Huang X, Molema G, King S, Watkins L, Edgington TS, Thorpe PE. Tumor infarction in mice by antibody directed targeting of tissue factor to tumor vasculature. *Science* 1997, **275**, 547–550.

22. Ran S, Gao B, Duffy S, Watkins L, Rote N, Thorpe PE. Infarction of solid Hodgkin's tumors in mice by antibody-directed targeting of tissue factor to tumor vasculature. *Cancer Res* 1998, **58**, 4646–4653.
23. Ohizumi I, Taniguchi K, Saito H, *et al*. Suppression of solid tumor growth by a monoclonal antibody against tumor vasculature in rats: involvement of intravascular thrombosis and fibrinogenisis. *Int J Cancer* 1999, **82**, 853–859.
24. Tsunoda S, Ohizumi I, Matsui J, *et al*. Specific binding of TES-23 antibody to tumor vascular endothelium in mice, rats and human cancer tissue: a novel drug carrier for cancer targeting therapy. *Br J Cancer* 1999, **81**, 1155–1161.
25. Taniguchi K, Harada N, Ohizumi I, *et al*. Recognition of human activated CD44 by tumor vasculature-targeted antibody. *Biochem Biophys Res Comm* 2000, **269**, 671–675.
26. Taniguchi K, Harada N, Ohizumi I, *et al*. Molecular cloning and characterization of antigens expressed on rat tumor vascular endothelial cells. *Int J Cancer* 2000, **86**, 799–805.
27. Kennel SJ, Lankford T, Hughes B, Hotchkiss JA. Quantitation of a specific murine lung endothelial cell protein, P112, with a double monoclonal antibody assay. *Lab Invest* 1983, **59**, 692–701.
28. Zalutsky MR, Narula AS. A method for the radiohalogenation of proteins resulting in decreased thyroid uptake of radioiodine. *Appl Radiat Isot* 1987, **38**, 1051–1055.
29. Koziorowski J, Henssen C, Weinreich R. A new convenient route to radioiodinated N-succinimidyl 3- and 4-iodobenzozte, two reagents for radioiodination of proteins. *Appl Radiat Isot* 1998, **49**, 955–959.
30. Kennel SJ, Mirzadeh S, Eckelman *et al*. Vascular targeted radioimmunotherapy with the α-emitter ^{211}At. *Nucl Med Biol*. Submitted for publication.
31. Brechbiel MW, Gansow OA. Synthesis of C-functionalised transcyclohexyldiethyleneaminopenta-acetic acids for labeling of monoclonal antibodies with the bismuth-212 α particle emitter. *J Chem Soc, Perkin Trans 1*, 1992, 1173–1178.
32. Kennel SJ, Mirzadeh S. Vascular targeting for radioimmunotherapy with ^{213}Bi. *Radiochimica Acta* 1997, **79**, 87–92.
33. Dadachova E, Chappell L, Brechbiel MW. Spectrophotometric method for determination of bifunctional macrocyclic ligand-protein conjugates. *Nucl Med Biol* 1999, **26**, 977–982.
34. Terzaghi-Howe M. Inhibition of carcinogen-altered rat tracheal cell proliferation by normal epithelial cells *in vivo*. *Carcinogenisis* 1987, **8**, 145–150.
35. Yuhas JM, Pazmino NH, Proctor JO, Toya RE. A direct relationship between immune competence and the subcutaneous growth rate of a malignant murine lung tumor. *Cancer Res* 1974, **34**, 722–728.
36. Friesel R, Maciag T. Internalization and degradation of heparin binding growth factor-I by endothelial cells. *Biochem Biophys Res Commun* 1988, **151**, 957–964.
37. Gerritsen ME, Shen C-P, Mchugh MC, *et al*. Activation-dependent isolation and culture of murine pulmonary microvascular endothelium. *Microcirculation* 1995, **2**, 151–163.
38. Kennel SJ, Foote LJ, Lankford PK, Johnson M, Mitchell T, Braslawsky GR. Direct binding of radioiodinated monoclonal antibody to tumor cells: significance of antibody purity and affinity for drug targeting or tumor imaging. *Hybridoma* 1983, **2**, 297–310.
39. McDevitt MR, Barendswaard E, Ma D, *et al*. An alpha-particle emitting antibody ([213Bi]J591) for radioimmunotherapy of prostate cancer. *Cancer Res* 2000, **60**, 6095–6100.
40. Kennel SJ, Chapell LL, Dadachova E, *et al*. Evaluation of ^{225}Ac for vascular targeted radioimmunotherapy of lung tumors. *Cancer Biother Radiopharm* 2000, **15**, 235–244.
41. Akabani G, Zalutsky MR. Microdosimetry of astatine-211 using histological images: application to bone marrow. *Radiat Res* 1997, **148**, 599–607.
42. Cooper MW, Robbins RC, Goldman CK, *et al*. Use of Yttrium-90 labeled antibody in primate xenograft transplantation. *Transplantation* 1990, **50**, 760–765.
43. Narayanan PK, Goodwin EH, Lehnert BE. Particles initiate biological production of superoxide anions and hydrogen peroxide in human cells. *Cancer Res* 1997, **57**, 3963–3973.